

# Structure and Reactivity of Mixed $\omega$ -Carboxyalkyl/Alkyl Monolayers on Silicon: ATR-FTIR Spectroscopy and Contact Angle Titration

Yong-Jun Liu, Neenah M. Navasero, and Hua-Zhong Yu\*

Department of Chemistry, Simon Fraser University, Burnaby,  
British Columbia V5A 1S6, Canada

Received September 29, 2003. In Final Form: March 3, 2004

The structure, reactivity, and acid–base properties of mixed monolayers prepared by photochemical reaction of hydrogen-terminated silicon with mixtures of ethyl undecylenate and  $n$ -alkenes were studied by ATR-FTIR spectroscopy and contact-angle measurements. The surface composition of the mixed monolayers and its correlation with the hydrolysis reactivity of terminal ethoxycarbonyl (ester) groups were investigated by systematically varying the mole fraction of ethyl undecylenate and the chain length of the unsubstituted alkenes in the binary deposition solution. It has been shown that the mole fraction of ester groups on the surface deviates only slightly from the mole fraction of ethyl undecylenate in the solution. The efficiency of ester hydrolysis under acidic conditions is significantly influenced by the monolayer structure, i.e., the surface density of ester groups and length of the unsubstituted alkyl chains. In addition, we find that mixed  $\omega$ -alkanoic acid/alkyl monolayers on silicon (prepared via hydrolysis) exhibit well-defined contact angle titration curves from which the surface acid dissociation constants were determined. The results were compared with the acid–base properties reported in the literature for carboxylic acid-terminated alkylsiloxane monolayers on hydroxylated silicon and for  $\omega$ -mercaptoalkanoic acid/alkanethiolate monolayers on gold. The weak  $pK_a$  dependence ( $\Delta pK_a \approx 1$ ) on the surface density of carboxylic acid groups and on the length of unsubstituted alkyl chains is attributed to variations of the microenvironment of the acid moieties. These experimental findings provide fundamental knowledge at the molecular level for the preparation of bioreactive surfaces of controlled reactivity on crystalline semiconductor substrates.

## Introduction

The development of synthetic routes to organic monolayers on silicon and subsequent structural investigations have been an active topic in the field of surface science<sup>1</sup> since Chidsey and co-workers reported their seminal work a decade ago.<sup>2</sup> In the past, organic monolayers were usually prepared by the reaction of organosilicon derivatives (such as alkylchlorosilanes, alkylalkoxysilanes, and alkylaminosilanes) with hydroxylated silicon surfaces.<sup>3</sup> The chemical reaction is the in situ formation of polysiloxane that is connected to surface silanol groups ( $\equiv\text{Si}-\text{OH}$ ) via Si–O–Si bonds. Besides the problems associated with the amorphous nature of the substrate ( $\text{SiO}_2$ –Si) and moisture sensitivity of the precursor molecules, the presence of a silicon dioxide thin film essentially blocks the electrical communication between the organic molecules and the silicon. In contrast, organic monolayers formed via Si–C bonds provide electronic coupling between organic functionalities and semiconductors without the interference of interfacial oxide thin films.<sup>1–2,4–9</sup>

We, and many others, have been interested in organic monolayers on silicon for fundamental studies of molec-

ular passivation, dielectrical performance, interfacial electron transport, and microscopic mechanical properties.<sup>6e,10–16</sup> Crystalline silicon is an attractive substrate for biochip fabrication (e.g., silicon-based DNA, protein, and peptide microarrays) because of its ultrahigh purity,

\* Correspondence should be addressed. E-mail: hzyu@sfu.ca.

(1) For recent reviews, see (a) Sieval, A. B.; Linke, R.; Zuilhof, H.; Sudhölter, E. J. R. *Adv. Mater.* **2000**, *12*, 1457–1460. (b) Wayner, D. D. M.; Wolkow, R. A. *J. Chem. Soc., Perkin Trans. 2* **2002**, 23–34. (c) Buriak, J. M. *Chem. Rev.* **2002**, *102*, 1271–1308.

(2) (a) Linford, M. R.; Chidsey, C. E. D. *J. Am. Chem. Soc.* **1993**, *115*, 12631–12632. (b) Linford, M. R.; Fenter, P.; Eisenberger, P. M.; Chidsey, C. E. D. *J. Am. Chem. Soc.* **1995**, *117*, 3145–3155. (c) Wagner, P.; Nock, S.; Spudich, J. A.; Volkmut, W. D.; Chu, S.; Cicero, R. L.; Wade, C. P.; Linford, M. R.; Chidsey, C. E. D. *J. Struct. Biol.* **1997**, *119*, 189–201.

(3) (a) Ulman, A. *An Introduction to Ultrathin Organic Films: From Langmuir–Blodgett to Self-Assembly*; Academic Press: New York, 1991; Part 3. (b) Ulman, A. *Chem. Rev.* **1996**, *96*, 1533–1554.

(4) Bansal, A.; Li, X.; Lauermann, I.; Lewis, N. S.; Yi, S. I.; Weinberg, W. H.; *J. Am. Chem. Soc.* **1996**, *118*, 7225–7226.

(5) (a) Henry de Villeneuve, C.; Pinson, J.; Bernard, M. C.; Allongue, P. *J. Phys. Chem. B* **1997**, *101*, 2415–2420. (b) Allongue, P.; Henry de Villeneuve, C.; Pinson, J.; Ozanam, F.; Chazalviel, J. N.; Wallart, X. *Electrochim. Acta* **1998**, *43*, 2791–2798.

(6) (a) Sieval, A. B.; Demirel, A. L.; Nissink, J. W. M.; Linford, M. R.; van der Maas, J. H.; de Jeu, W. H.; Zuilhof, H.; Sudhölter, E. J. R. *Langmuir* **1998**, *14*, 1759–1768. (b) Sieval, A. B.; Vleeming, V.; Zuilhof, H.; Sudhölter, E. J. R. *Langmuir* **1999**, *15*, 8288–8291. (c) Sieval, A. B.; Linke, R.; Heij, G.; Meijer, G.; Zuilhof, H.; Sudhölter, E. J. R. *Langmuir* **2001**, *17*, 7554–7559. (d) de Smet, L. C. P. M.; Stork, G. A.; Hurenkamp, G. H. F.; Sun, Q.-Y.; Topal, H.; Vronen, P. J. E.; Sieval, A. B.; Wright, A.; Visser, G. M.; Zuilhof, H.; Sudhölter, E. J. R. *J. Am. Chem. Soc.* **2003**, *125*, 13916–13917. (e) Sieval, A. B.; Huisman, C. L.; Schonecker, A.; Schuurmans, F. M.; van der Heide, A. S. H.; Goossens, A.; Sinke, W. C.; Zuilhof, H.; Sudhölter, E. J. R. *J. Phys. Chem. B* **2003**, *107*, 6846–6852.

(7) (a) Boukherroub, R.; Morin, S.; Bensebaa, F.; Wayner, D. D. M. *Langmuir* **1999**, *15*, 3831–3835. (b) Boukherroub, R.; Wayner, D. D. M. *J. Am. Chem. Soc.* **1999**, *121*, 11513–11515.

(8) (a) Fidélis, A.; Ozanam, F.; Chazalviel, J.-N. *Surf. Sci.* **2000**, *444*, L7–L10. (b) Teyssot, A.; Fidélis, A.; Fellah, S.; Ozanam, F.; Chazalviel, J.-N. *Electrochim. Acta* **2002**, *47*, 2565–2571.

(9) Yates, J. T., Jr. *Science* **1998**, *279*, 335–336, and references therein.

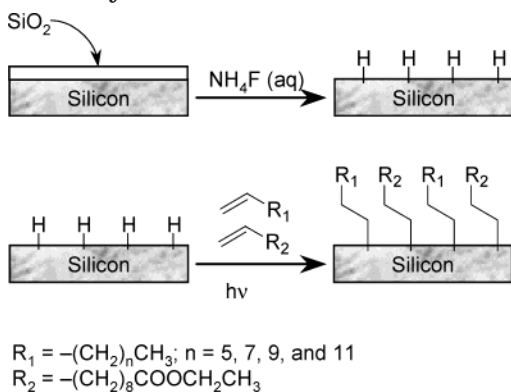
(10) (a) Bansal, A.; Lewis, N. S. *J. Phys. Chem. B* **1998**, *102*, 1067–1070. (b) Haber, J. A.; Lauermann, I.; Michalak, D.; Vaid, T. P.; Lewis, N. S. *J. Phys. Chem. B* **2000**, *104*, 9947–9950. (c) Webb, L. J.; Lewis, N. S. *J. Phys. Chem. B* **2003**, *23*, 5404–5412.

(11) (a) Yu, H. Z.; Morin, S.; Wayner, D. D. W.; Allongue, P.; Henry de Villeneuve, C. *J. Phys. Chem. B* **2000**, *104*, 11157–11161. (d) Yu, H. Z.; Boukherroub, R.; Morin, S.; Wayner, D. D. M. *Electrochem. Commun.* **2000**, *2*, 562–566.

(12) (a) Barrelet, C. J.; Robinson, D. B.; Cheng, J.; Hunt, T. P.; Quate, C. F.; Chidsey, C. E. D. *Langmuir* **2001**, *17*, 3460–3465. (b) Cheng, J.; Robinson, D. B.; Cicero, R. L.; Eberspacher, T.; Barrelet, C. J.; Chidsey, C. E. D. *J. Phys. Chem. B* **2001**, *105*, 10900–10904.

(13) (a) Wei, F.; Zhao, X. S. *Thin Solid Films* **2002**, *408*, 286–290. (b) Zhao, X. S.; Wei, F. Private communications 2000.

**Scheme 1. The Preparation of Mixed  $\omega$ -ethoxycarbonyl/Alkyl Monolayers on Silicon Formed via Photochemical Reactions of Hydrogen-terminated Silicon with Mixtures of Ethyl Undecylenate and Different  $n$ -Alkenes**



well-defined structure, and the opportunity to take full advantage of existing microelectronic technology.<sup>17–19</sup> In practice, simple and efficient strategies for the attachment of functional groups (such as COOH, NH<sub>2</sub> or OH) and the systematic variation of their surface densities in a predictable and accurately determinable manner are of primary importance for the immobilization of biological macromolecules and the relief of steric congestion on the chip surface.<sup>7b</sup> The reagents and reaction conditions chosen should be powerful enough to overcome significant kinetic barriers to induce the desired surface transformations, but still mild enough to be compatible with the surface functionalities, supporting monolayers, and underlying substrates.<sup>20</sup>

Several synthetic methods have been employed to prepare organic monolayers on silicon surfaces including thermal, catalyzed, and photochemical reactions with alkenes,<sup>2,6–7</sup> thermal reactions with Grignard reagents,<sup>7a</sup> and electrochemical grafting of aryl diazonium ions and Grignard reagents.<sup>5,8</sup> Alkyl monolayers on silicon may also be prepared by the reaction of alkylmagnesium or alkyl-lithium reagents with halogenated silicon surfaces.<sup>4,10</sup> The photochemical reaction of  $n$ -alkenes and their derivatives with hydrogen-terminated silicon surfaces is one of the most popular methods because of its simplicity, mild reaction conditions, and high quality of monolayers.<sup>2c,6d,7</sup> As illustrated in Scheme 1, this two-step surface modification protocol is technically simple: preparation of the hydrogen-terminated silicon surface by etching in deoxy-genated NH<sub>4</sub>F (aqueous, 40%) solution, followed by ultra-

violet (UV) irradiation in the presence of neat alkenes or their solutions. By using two different terminally substituted alkenes, mixed  $\omega$ -functionalized monolayers can be readily prepared by this method.

One of the successful examples along this line is the formation of  $\omega$ -alkoxycarbonyl (ester) terminated monolayers that can be converted to carboxylic acid (COOH) terminated surfaces.<sup>6a,7b</sup> The covalent bond between alkyl chain and silicon provides enhanced stability but restricts the types of functional groups that can be incorporated in the monolayer. For example, closely packed alkyl monolayers terminated with COOH groups cannot be directly prepared from  $\omega$ -carboxy-1-alkenes due to the reactivity of COOH with hydrogen-terminated silicon,<sup>6a,13b,21</sup> which competes with the preferred reaction between CH<sub>2</sub>=CH- and the substrate. Sieval et al. made pioneering contributions to the study of thermal reactions of ester-terminated alkenes with H-Si(100) and hydrolysis of thus formed monolayers. However, the unsatisfactory signal-to-noise ratio in the carbonyl region of their FTIR spectra did not permit quantitation.<sup>6a</sup> Boukherroub and Wayner communicated their experimental results with photochemically prepared ester-terminated monolayers on silicon, with the focus on various functional group transformations including acid-catalyzed ester hydrolysis.<sup>7b</sup> Hamers et al.<sup>17a</sup> and Zhao et al.<sup>13a,19</sup> recently reported different methods for the hydrolysis of terminal ester groups in their related studies.

Surfaces with covalently attached carboxylic acids have been traditionally created by oxidizing polymer surfaces,<sup>22</sup> functionalizing alkanesiloxane monolayers formed on hydroxylated substrates,<sup>23</sup> or adsorbing COOH-terminated organosulfur molecules on gold.<sup>24</sup> Being model systems for studies of wettability, adsorption of colloids and proteins, and attachment of DNA strands, these surfaces have been analyzed by a variety of techniques including spectroscopic,<sup>25</sup> electrochemical,<sup>26</sup> and wetting (contact angle) measurements.<sup>27,28</sup> Due to the high sensitivity and simplicity of operation, contact-angle measurements have been widely used to study alkanethiolate monolayers on gold, such as to monitor the formation process,<sup>29</sup> to follow the step-by-step modification,<sup>30</sup> and to evaluate kinetic data for surface reactions.<sup>31</sup> Of particular interest, Whitesides and co-workers have pioneered the use of the

(14) (a) Kim, N. Y.; Laibinis, P. E. *J. Am. Chem. Soc.* **1999**, *121*, 7162–7163. (b) Vermeir, I. E.; Kim, N. Y.; Laibinis, P. E. *App. Phys. Lett.* **1999**, *74*, 3860–3862.

(15) Zhang, L. Z.; Li, L. Y.; Chen, S. F.; Jiang, S. Y. *Langmuir* **2002**, *18*, 5448–5456.

(16) (a) Liu, Y. J.; Yu, H. Z. *ChemPhysChem* **2002**, *3*, 799–802. (b) Liu, Y. J.; Yu, H. Z. *ChemPhysChem* **2003**, *4*, 335–342. (c) Liu, Y. J.; Yu, H. Z. *J. Phys. Chem. B* **2003**, *107*, 7803–7811.

(17) (a) Strother, T.; Cai, W.; Zhao, X. S.; Hamers, R. J.; Smith, L. M. *J. Am. Chem. Soc.* **2000**, *122*, 1205–1209. (b) Strother, T.; Hamers, R. J.; Smith, L. M. *Nucleic Acids Res.* **2000**, *28*, 3535–3541. (c) Zhang, L.; Strother, T.; Cai, W.; Cao, X. P.; Smith, L. M.; Hamers, R. J. *Langmuir* **2002**, *18*, 788–796.

(18) Pike, A. R.; Lie, L. H.; Eagling, R. A.; Ryder, L. C.; Patole, S. N.; Connolly, B. A.; Horrocks, B. R.; Houlton, A. *Angew. Chem., Int. Ed. Engl.* **2002**, *41*, 615–617.

(19) (a) Wei, F.; Sun, B.; Liao, W.; Ouyang, J. H.; Zhao, X. S. *Biosensors & Bioelectronics* **2003**, *18*, 1149–1155. (b) Wei, F.; Sun, B.; Guo, Y.; Zhao, X. S. *Biosensors & Bioelectronics* **2003**, *18*, 1157–1163.

(20) Fryxell, G. E.; Rieke, P. C.; Wood, L. L.; Engelhard, M. H.; Williford, R. E.; Graff, G. L.; Campbell, A. A.; Wiacek, R. J.; Lee, L.; Halverson, A. *Langmuir* **1996**, *12*, 5064–5075.

(21) (a) Lee, E. J.; Ha, J. S.; Sailor, M. J. *J. Am. Chem. Soc.* **1995**, *117*, 8295–8296. (a) Lee, E. J.; Bitner, T. W.; Ha, J. S.; Shane, M. J.; Sailor, M. J. *J. Am. Chem. Soc.* **1996**, *118*, 5375–5382.

(22) For examples, see (a) Holmes-Farley, S. R.; Reamey, R. H.; McCarthy, T. J.; Deutch, J.; Whitesides, G. M. *Langmuir* **1985**, *1*, 725–740. (b) Holmes-Farley, S. R.; Bain, C. D.; Whitesides, G. M. *Langmuir* **1988**, *4*, 921–937.

(23) For examples, see (a) Haller, I. *J. Am. Chem. Soc.* **1978**, *100*, 8050–8055. (b) Pomerantz, M.; Segmuller, A.; Netzer, L.; Sagiv, J. *Thin Solid Films* **1985**, *132*, 153–162. (c) Wasserman, S. R.; Tao, Y. T.; Whitesides, G. M. *Langmuir* **1989**, *5*, 1074–1087.

(24) For examples, see (a) Nuzzo, R. G.; Allara, D. L. *J. Am. Chem. Soc.* **1983**, *105*, 4481–4483. (b) Porter, M. D.; Bright, T. B.; Allara, D. L.; Chidsey, C. E. D. *J. Am. Chem. Soc.* **1987**, *109*, 3559–3568. (c) Laibinis, P. E.; Whitesides, G. M. *J. Am. Chem. Soc.* **1992**, *114*, 1990–1995.

(25) Sun, L.; Crooks, R. M. *Langmuir* **1993**, *9*, 1775–1780.

(26) Malem, F.; Mandler, D. *Anal. Chem.* **1993**, *65*, 37–41.

(27) (a) Bain, C. D.; Whitesides, G. M. *Langmuir* **1989**, *5*, 1370–1378. (b) Lee, T. R.; Carey, R. I.; Biebuyck, H. A.; Whitesides, G. M. *Langmuir* **1994**, *10*, 741–749.

(28) Creager, S. E.; Clarke, J. *Langmuir* **1994**, *10*, 3675–3683.

(29) For examples, see (a) Bain, C. D.; Troughton, E. B.; Tao, Y. T.; Evall, J.; Whitesides, G. M.; Nuzzo, R. G. *J. Am. Chem. Soc.* **1989**, *111*, 321–335. (b) Yu, H. Z.; Zhao, J. W.; Wang, Y. Q.; Liu, Z. F. *Mol. Cryst. Liq. Cryst. A* **1997**, *294*, 107–112. (c) Liao, S.; Shnidman, Y.; Ulman, A. *J. Am. Chem. Soc.* **2000**, *122*, 3688–3694.

(30) Yu, H. Z.; Zhao, J. W.; Wang, Y. Q.; Cai, S. M.; Liu, Z. F. *J. Electroanal. Chem.* **1997**, *438*, 221–224.

(31) Banks, J. T.; Yu, T. T.; Yu, H. Z. *J. Phys. Chem. B* **2002**, *106*, 3538–3542.



contact angle titration method, i.e., determination of the contact angles of a series of buffered water droplets as a function of the pH of the droplet, for studying acid–base reactions of  $\omega$ -carboxy-terminated alkanethiolate monolayers on gold.<sup>27</sup> Creager and Clarke have characterized mixed  $\omega$ -mercaptoalkanoic acid/alkanethiolate monolayers on gold by developing a special pretreatment procedure, the so-called nonreactive spreading protocol,<sup>28</sup> which gives ideal titration curves (exhibiting a smooth transition between plateau regions at low and high pH). Wasserman et al. reported contact angle titration studies of COOH-terminated alkylsiloxane monolayers on hydroxylated silicon substrates.<sup>23c</sup>

The present research aims at an assessment of the factors determining the formation and reactivity of mixed  $\omega$ -carboxyalkyl/alkyl monolayers on silicon and discusses the fundamental principles underlying the demonstrated applications of these molecularly tailored semiconductor surfaces. This comprehensive report describes our ATR-FTIR spectroscopic and contact angle studies of the formation of mixed  $\omega$ -carboxyalkyl/alkyl monolayers on silicon, the effects of molar ratio and chain length of precursor alkenes and of reaction conditions (acidic vs basic) on the efficiency of ester hydrolysis on surfaces, and the acid–base properties of the mixed monolayers upon hydrolysis. Knowledge of the exact ionization state of the carboxylic moieties is of critical importance for the selection of optimal reaction conditions for the immobilization of biological molecules.<sup>17–19</sup>

## Experimental Section

**Materials.** All chemicals were of reagent grade or the highest available commercial-grade quality and used as received unless otherwise stated. Deionized water ( $>18.3\text{ M}\Omega\cdot\text{cm}$ ) was obtained from a Barnstead EasyPure UV/UF compact water system (Dubuque, IA). 1-Octene (98%), 1-decene ( $>95\%$ ), 1-dodecene (95%), 1-tetradecene (92%), and ethyl undecylenate (97%) were purchased from Aldrich (Milwaukee, WI); tetrahydrofuran (THF) and 1,1,1-trichloroethane (99.5%) from Caledon Laboratories Ltd. (Georgetown, ON); ammonium fluoride (40%), sulfuric acid (96%), and hydrogen peroxide (30%) from GEM Microelectronic Materials Inc. (Chandler, AZ).

All alkenes were redistilled from sodium under reduced pressure ( $\sim 20\text{--}30\text{ Torr}$ ); ethyl undecylenate was purified by passing through an activated  $\text{Al}_2\text{O}_3$  column.

**Preparation of Silicon Substrate.** Silicon (111) wafers ( $0.5\text{--}5.0\text{ }\Omega\cdot\text{cm}$ , n-type, Virginia Semiconductor Inc.) were cut into strips ( $15 \times 20\text{ mm}^2$ ). They were initially cleaned in “piranha” solution, a 3:1 mixture of concentrated  $\text{H}_2\text{SO}_4$  and  $\text{H}_2\text{O}_2$  (30%) heated to about  $90\text{ }^\circ\text{C}$  for 30 min (CAUTION: “piranha” solution reacts violently with organic materials, it must be handled with extreme care), followed by copious rinsing with deionized water. As shown in Scheme 1, cleaned silicon samples were etched with ppb grade  $\text{NH}_4\text{F}$  (40% aqueous solution, deoxygenated for at least 15 min by bubbling argon) to remove native oxide and obtain hydrogen-terminated silicon (H–Si). The Si (111) attenuated total reflectance (ATR) crystals ( $25 \times 5 \times 1\text{ mm}^3$ , Harrick Scientific Inc.) were cleaned by the standard RCA procedure,<sup>32</sup> prior to the etching steps outlined above.

**Formation of Alkyl Monolayers on Silicon.** The fresh H–Si sample was transferred under argon into a Schlenk tube containing  $2\text{--}3\text{ mL}$  of a deoxygenated neat alkene or a mixture of  $n$ -alkene and ethyl undecylenate and irradiated in a UV photoreactor (350 nm, Model: LZC-TIM300, Luzchem Research Inc., Ottawa, ON) for 3 to 5 h. The modified silicon substrate was then rinsed at room temperature with THF, deionized water, and finally 1,1,1-trichloroethane before characterization. The hydrolysis of ester-terminated monolayers to produce carboxylic acid (COOH)-terminated silicon surfaces was carried out by immersion in  $2.0\text{ M HCl}$  at  $70\text{ }^\circ\text{C}$  for 2 h or by dipping the sample

into  $0.25\text{ M}$  potassium *tert*-butoxide solution in DMSO for 3 min, and then washing with  $\text{HCl}$  solution ( $2.0\text{ M}$ ).

**Surface Characterization.** Attenuated total reflectance (ATR)-FTIR spectra were recorded using a Nicolet Nexus-IR 560 spectrometer equipped with an MCT detector cooled with liquid nitrogen. The ATR crystals were mounted in a dry-air purged sample chamber with the light focused normal to one of the  $45^\circ$  bevels. Background spectra were obtained using freshly prepared oxidized silicon surfaces that give more reproducible results than hydrogen-terminated silicon.<sup>7b</sup> This is possibly due to the fact that H–Si is easily contaminated and undergoes gradual oxidation in air.<sup>33</sup> The spectra were collected for 1000 scans at a  $2.0\text{ cm}^{-1}$  resolution. They were measured in the range of  $4000\text{--}1500\text{ cm}^{-1}$ , which is limited by the high absorbance of silicon ATR crystals below  $1500\text{ cm}^{-1}$ . No corrections were made for either water vapor or atmospheric  $\text{CO}_2$ . In most cases, a linear baseline correction was carefully applied.

Wetting measurements were performed on an AST Optima contact angle system at ambient conditions ( $18\text{--}22\text{ }^\circ\text{C}$ ,  $30\text{--}35\%$  relative humidity) using a horizontal light beam to illuminate the liquid droplet. The contact angles reported are thermodynamic equilibrated values of sessile liquid drops of either pure water or buffer solutions. For contact angle titration measurements, the silicon sample was immersed in the buffer solution before the contact angle of that specific buffer was recorded. At least five  $1.0\text{--}2.0\text{-}\mu\text{L}$  drops of each buffer were measured and the average was taken for each point on a pH titration curve. The ionic strength was  $0.01\text{ M}$  for all buffer solutions except those at very high and low pH. The buffer solutions were prepared according to Creager et al.<sup>28</sup> as follows: pH 0–1, perchloric acid; pH 2–3, phosphoric acid/sodium phosphate monobasic; pH 4–5, acetic acid/sodium acetate; pH 6–8, sodium phosphate monobasic/sodium phosphate dibasic; pH 9–11, sodium bicarbonate/sodium carbonate; pH 12, sodium phosphate dibasic/sodium phosphate tribasic. Exact pH values for the buffer solutions were recorded before and after the contact angle measurements.

## Results and Discussion

Ultraviolet irradiation of freshly prepared H–Si in the presence of alkenes results in the formation of alkyl monolayers covalently bound to silicon via Si–C bonds.<sup>2c,7</sup> Reaction time was typically from 3 to 5 h, and no dependence of the film quality on the irradiation duration was discernible. The silicon surfaces modified with  $n$ -alkyl monolayers are more hydrophobic as shown by larger contact angles obtained with  $\text{H}_2\text{O}$  ( $104 \pm 2^\circ$  for 1-dodecyl monolayers) compared to hydrogen-terminated silicon ( $82 \pm 5^\circ$ ). Mixed monolayers were formed by using either ethyl undecylenate and 1-dodecene at different mole ratios or equimolar mixtures of ethyl undecylenate and an  $n$ -alkene with varied chain length (Scheme 1). Before the spectroscopic studies, the surface homogeneity of the modified silicon surface was confirmed by atomic force microscopy (AFM) images.<sup>34</sup> In the following sections, we will first focus on the structural characterization, then on the hydrolysis of pure and mixed  $\omega$ -ethoxycarbonyl-terminated monolayers under varied reaction conditions, and finally on the contact angle titrations.

**Structure of Mixed  $\omega$ -Ethoxycarbonyl/Alkyl Monolayers on Silicon.** ATR-FTIR spectroscopy has been proved to be a powerful tool to study the chain conformation and orientation,<sup>2,6</sup> to determine the coverage and packing,<sup>7</sup> and to monitor the surface chemistry<sup>6a,7b,35–36</sup> of organic monolayers formed on different semiconductor surfaces. Figure 1 shows the ATR-FTIR spectra of mixed monolayers on silicon formed by the reactions of H–Si

(33) (a) Ye, S.; Ichihara, T.; Uosaki, K. *Appl. Phys. Lett.* **1999**, *75*, 1562–1564. (b) Liu, Y. J.; Waugh, D. M.; Yu, H. Z. *Appl. Phys. Lett.* **2002**, *81*, 4967–4969.

(34) The AFM images show the same features as reported for  $\text{Si-C}_{10}\text{H}_{2n+1}$  in ref 7, i.e., atomically flat terraces that are free of etch pits and stable in air.

(32) Kern, W.; Puotinen, D. A. *RCA Rev.* **1970**, *31*, 188–206.

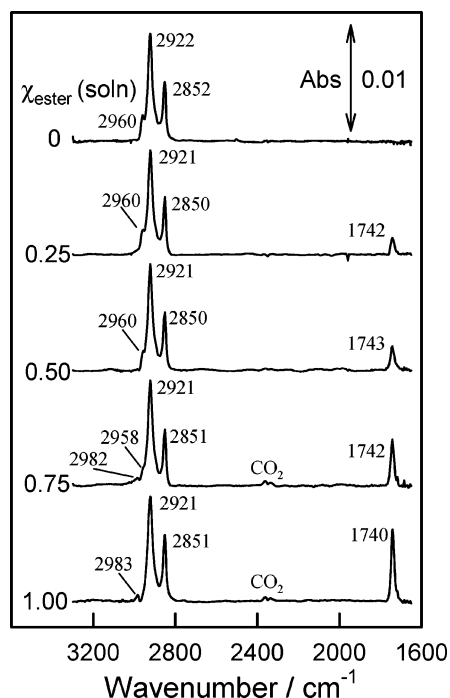


**Figure 1.** FTIR spectra of mixed  $\omega$ -ethoxycarbonyl/alkyl monolayers on silicon formed by the reaction of hydrogen-terminated silicon (ATR crystals) with mixtures of ethyl undecylenate and 1-dodecene.  $\chi_{\text{ester}}(\text{soln})$  refers to the mole fraction of ethyl undecylenate in the binary deposition solution.

(ATR plates) with solutions containing ethyl undecylenate and 1-dodecene at different molar ratios. The positions of the major bands are listed for each spectrum together with the corresponding mole fraction of ethyl undecylenate in solution,  $\chi_{\text{ester}}(\text{soln})$ .

As shown in Figure 1, two regions (CH stretching between 3200 and 2700  $\text{cm}^{-1}$  and carbonyl stretching around 1740  $\text{cm}^{-1}$ ) are characteristic besides the atmospheric  $\text{CO}_2$  bands (2335 and 2362  $\text{cm}^{-1}$ ). The band at 2958–60  $\text{cm}^{-1}$  (discernible for  $\chi_{\text{ester}} < 0.75$ ) is assigned to the  $\text{CH}_3$  asymmetric in-plane CH stretching mode; its intensity decreases with increasing  $\chi_{\text{ester}}(\text{soln})$ . This band reappears at 2983  $\text{cm}^{-1}$  for monolayers with a high concentration of ethyl undecylenate in solution ( $\chi_{\text{ester}} > 0.75$ ), but it originates from vibrations of  $-\text{OCH}_2\text{CH}_3$  instead of the methyl groups of 1-dodecyl chains.<sup>37</sup> The bands at 2921–2  $\text{cm}^{-1}$  and 2850–1  $\text{cm}^{-1}$  are assigned to the  $\nu_a(\text{CH}_2)$  and  $\nu_s(\text{CH}_2)$  stretching modes, respectively. These two modes were normally selected for structural interpretation due to their distinct features and the minimal overlap with other absorption bands.

Comparison of the IR spectra of pure and mixed monolayers on silicon shown in Figure 1 leads to two immediate conclusions. First, the close agreement of the peak positions at different values of  $\chi_{\text{ester}}(\text{soln})$ , which is consistent with literature data,<sup>6a,7b</sup> demonstrates that the structural integrity of the alkyl chains is not significantly affected by the molar ratio of the two precursor molecules. Second, the  $\text{CH}_2$  stretching absorption intensities at different  $\chi_{\text{ester}}(\text{soln})$  are very close to each other, indicating that the photochemical reaction of either pure or binary

solutions of unsubstituted and substituted alkenes yields uniform monolayers with similar coverage on silicon. The position of the peak for the  $\nu_a(\text{CH}_2)$  mode in Figure 1 provides insights into the intermolecular environment of the alkyl chains within the monolayers formed under different conditions. Snyder et al. have shown that it is a sensitive indicator of the extent of lateral interactions between long alkyl chains.<sup>38</sup> It has been confirmed previously that the peak position of  $\nu_a(\text{CH}_2)$  at 2921–2  $\text{cm}^{-1}$  indicates a dense packing of the alkyl chains in these monolayers by comparison with those of the solid crystal phase (2920  $\text{cm}^{-1}$ ) and the liquid state (2928  $\text{cm}^{-1}$ ).<sup>6,7</sup> We note that alkyl monolayers formed on silicon are not as ordered and closely packed as long-chain alkanethiolate monolayers on gold, in which  $\nu_a(\text{CH}_2)$  appears at an even shorter wavenumber (e.g., 2917  $\text{cm}^{-1}$  for  $\text{CH}_3(\text{CH}_2)_{17}\text{S}-\text{Au}$ ),<sup>24b</sup> partially due to the lower surface coverage limited by the crystalline structure of silicon.<sup>2b,7b</sup> Chidsey and co-workers noted that since the distance between silicon atoms on the Si(111) surface is 3.84 Å and the diameter of an alkyl chain is about 4.2 Å, complete  $1 \times 1$  coverage of the silicon surface is spatially not feasible.<sup>2b</sup> Experimental measurements by ellipsometry and X-ray reflectivity provided a tilt angle of about 35° from the surface normal for the monolayers prepared by photoreactions of  $n$ -alkenes with silicon, which is consistent with a surface coverage of about 50%.<sup>2b,6a</sup> Nevertheless, the identical frequencies of the  $\nu_a(\text{CH}_2)$  mode within experimental error ( $\pm 2 \text{ cm}^{-1}$ ) reveal that the quality of the mixed monolayers formed on silicon are as high as of those prepared from pure  $n$ -alkenes in terms of the chain conformation, orientation, and packing. In fact, the same conclusion can be drawn from the positions of the  $\nu_s(\text{CH}_2)$  and  $\nu_a(\text{CH}_3)$  stretching bands at 2850–1  $\text{cm}^{-1}$  and 2958–60  $\text{cm}^{-1}$ , respectively.

It should be noted that the most significant difference among the spectra shown in Figure 1 is the band at 1740–3  $\text{cm}^{-1}$  that can be unambiguously assigned to the C=O stretch of the ester groups.<sup>37</sup> As expected, its intensity increases with the increased mole fraction of ethyl undecylenate in solution. The high quality of these FTIR spectra (high signal-to-noise ratio and unambiguous peak assignments) gives us an opportunity to determine the surface compositions of the mixed monolayers. To minimize the influence of absolute intensity, we plotted the ratio of the  $\nu(\text{C}=\text{O})$  and  $\nu_a(\text{CH}_2)$  intensities,  $A_{1740}/A_{2922}$ , as a function of  $\chi_{\text{ester}}(\text{soln})$ , which shows the expected monotonic increase (Figure 2A). Considering the fact that these monolayers have almost identical surface coverage/packing density as mentioned above, the surface mole fraction,  $\chi_{\text{ester}}(\text{surf})$ , can be derived from the results in Figure 2A by normalizing the values of  $A_{1740}/A_{2922}$  of mixed monolayers to that of the pure ester-terminated monolayer (the spectrum corresponding to  $\chi_{\text{ester}} = 1.0$  in Figure 1).

As shown in Figure 2B, the mole fraction on the surface deviates only slightly from that in the binary solutions, which is consistent with the results reported by others for similar systems,<sup>7b,13a</sup> which is in sharp contrast to the clearly preferred adsorption of long-chain  $n$ -alkanethiols over  $\omega$ -substituted alkanethiols when mixed monolayers are formed on gold.<sup>39</sup> Differing from the Si–C covalent bonding between the alkyl chains and silicon, alkanethiolate monolayers formed on gold through relatively weaker

(35) Cheng, S. S.; Scherson, D. A.; Sukenik, C. N. *Langmuir* **1995**, *11*, 1190–1195.

(36) Pomerantz, M.; Segmuller, A.; Netzer, L.; Sagiv, J. *Thin Solid Films* **1985**, *132*, 153–162.

(37) Lin-Vien, D.; Colthup, N. B.; Fateley, W. G.; Grasselli, J. G. *The Handbook of Infrared and Raman Characteristic Frequencies of Organic Molecules*; Academic Press: San Diego, CA, 1991; pp 134–141.

(38) (a) Snyder, R. G.; Strauss, H. L.; Elliger, C. A. *J. Phys. Chem.* **1982**, *86*, 5145–5150. (b) Snyder, R. G.; Maroncelli, M.; Strauss, H. L.; Hallmark, V. M. *J. Phys. Chem.* **1986**, *90*, 5623–5630.

(39) (a) Bain, C. D.; Whitesides, G. M. *J. Am. Chem. Soc.* **1988**, *110*, 6560–6561. (b) Bain, C. D.; Evall, J.; Whitesides, G. M. *J. Am. Chem. Soc.* **1989**, *111*, 7155–7164.

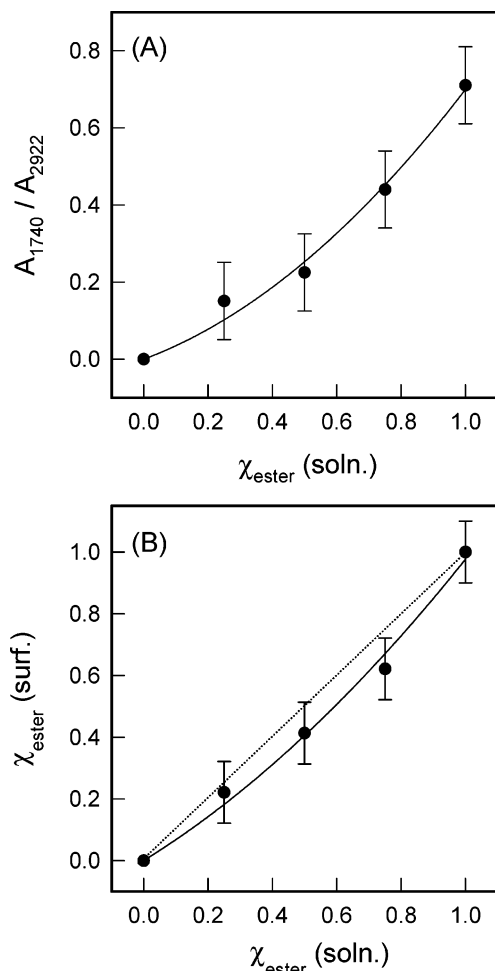


**Figure 2.** (A) Absorbance ratio  $\nu(\text{C}=\text{O})/\nu_{\text{a}}(\text{CH}_2)$  of Figure 1; (B) Surface mole fraction,  $\chi_{\text{ester}}(\text{surf})$ , as a function of the mole fraction of ethyl undecylenate in the binary deposition solution,  $\chi_{\text{ester}}(\text{soln})$ . The solid lines are included simply to guide the eye. The dashed line in (B) corresponds to the nonselective reaction model (i.e., assuming that the surface composition is identical to that of the deposition solution).

Au-S interactions that are significantly influenced by intermolecular forces between the adsorbates.<sup>3</sup> More importantly, the results presented in Figure 2B demonstrate that the surface density of functional groups on silicon is predictable and can be controlled by simply varying the composition of the binary solution for reaction.

Wetting measurements are more sensitive to the surface properties (the surface density and distribution of functional groups), which provide an easy alternative method to study organic monolayers. The measured contact angles using sessile drops of pure water on monolayers prepared from pure *n*-alkenes ( $104 \pm 2^\circ$  for 1-dodecyl monolayers) are consistent with those reported previously.<sup>6a,11a</sup> In contrast to the high hydrophobicity of *n*-alkyl monolayers on silicon compared to hydrogen-terminated silicon ( $82 \pm 3^\circ$ ), the introduction of ester groups to the surfaces does not change the apparent wetting properties significantly ( $82 \pm 4^\circ$ ). Nevertheless, the correlation of the water contact angle with mole fraction of ethyl undecylenate in solution,  $\chi_{\text{ester}}(\text{soln})$ , is distinct (Figure 3A): with increased  $\chi_{\text{ester}}(\text{soln})$ , the surface becomes more hydrophilic as indicated by the decreased contact angles.

If the silicon surface modified with mixed monolayers is considered to consist of two types of domains, i.e., methyl and ester groups, the intrinsic contact angles with respect

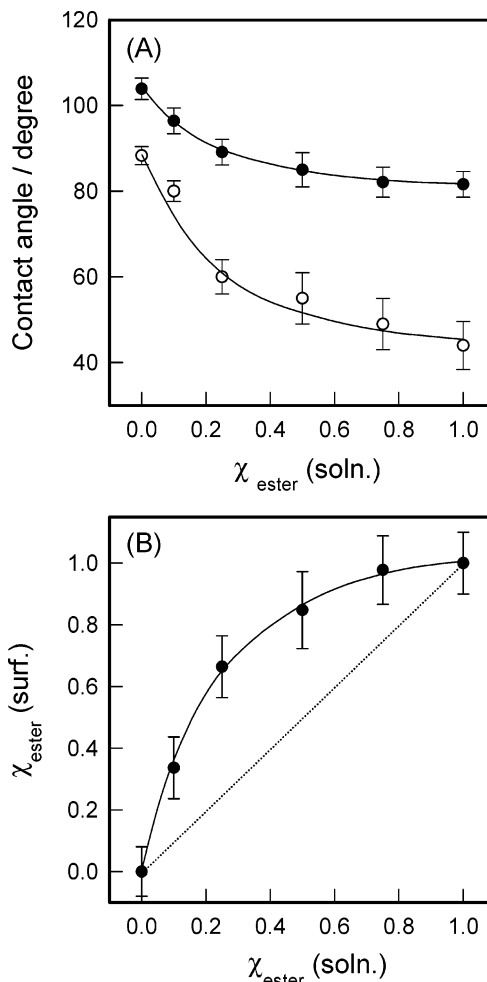


**Figure 3.** (A) Water contact angles of mixed monolayers (prepared from mixtures of 1-dodecene and ethyl undecylenate) before (closed circles) and after hydrolysis (open circles) as a function of the mole fraction of ethyl undecylenate in solution,  $\chi_{\text{ester}}(\text{soln})$ ; (B) surface mole fraction of ethyl undecylenate,  $\chi_{\text{ester}}(\text{surf})$  vs  $\chi_{\text{ester}}(\text{soln})$ , which was determined from the water contact angles of mixed SAMs using Cassie's equation. The solid lines are included simply to guide the eye. The dashed line in panel B corresponds to the nonselective attachment model of the two alkenes.

to water being  $\theta_{\text{me}}$  and  $\theta_{\text{ester}}$ , the surface mole fraction of esters,  $\chi_{\text{ester}}(\text{surf})$  can be determined from Cassie's law<sup>40</sup>

$$\cos \theta = \chi_{\text{ester}}(\text{surf}) \cos \theta_{\text{ester}} + [1 - \chi_{\text{ester}}(\text{surf})] \cos \theta_{\text{me}} \quad (1)$$

Rearrangement of eq 1 gives

$$\chi_{\text{ester}}(\text{surf}) = \frac{\cos \theta - \cos \theta_{\text{me}}}{\cos \theta_{\text{ester}} - \cos \theta_{\text{me}}} \quad (2)$$

Figure 3B shows the dependence of  $\chi_{\text{ester}}(\text{surf})$ , calculated from eq 2, on the mole fraction of ethyl undecylenate in solution,  $\chi_{\text{ester}}(\text{soln})$ . Although there is a reasonable increase of  $\chi_{\text{ester}}(\text{surf})$  with increasing  $\chi_{\text{ester}}(\text{soln})$ , the correlation between surface and solution composition based on wetting measurements is clearly different from that derived from the spectroscopic data (Figure 2B). We believe that the spectroscopic measurements provide more reliable information than the wetting studies. Cassie's interpretation of chemically heterogeneous surfaces is

(40) Cassie, A. B. D. *Discuss. Faraday Soc.* **1948**, 3, 11–16.



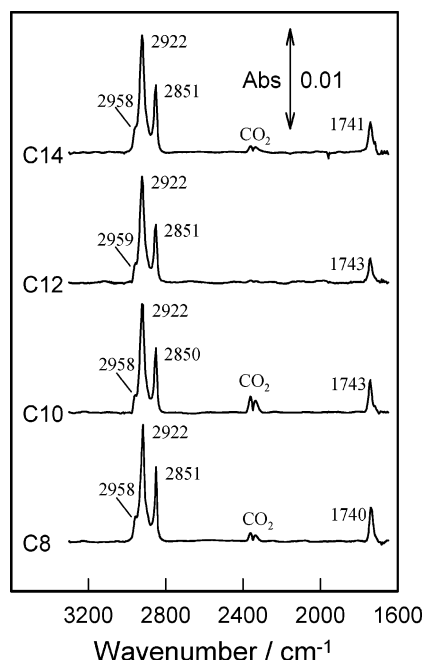
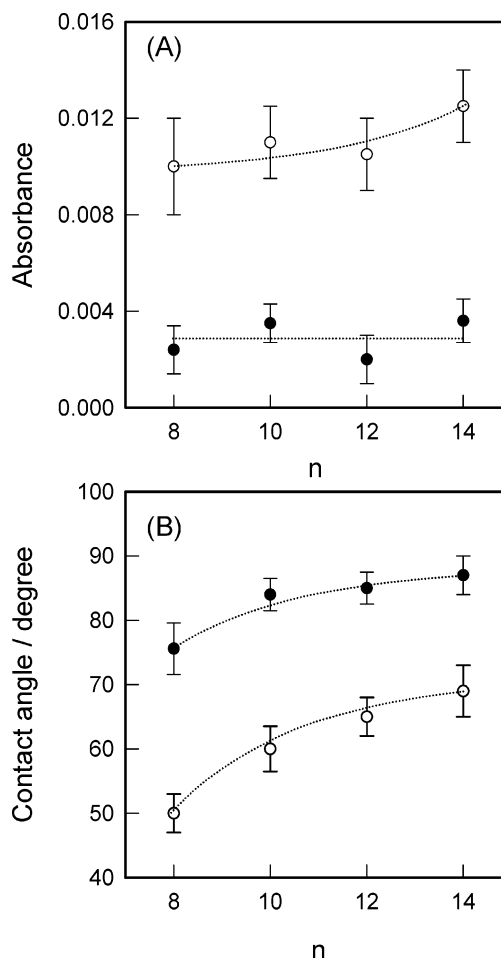


**Figure 4.** FTIR spectra of mixed monolayers prepared by the photochemical reaction of silicon ATR crystals with equimolar mixtures of ethyl undecylenate and 1-octene (C8), 1-decene (C10), 1-dodecene (C12), and 1-tetradecene (C14), respectively.

debatable, particularly when the surface contains two totally dispersed species without significant formation of domain structures. Unlike the formation of alkanethiolate monolayers on gold in which reconstruction induced by intermolecular forces plays an important role in determining the final monolayer structure and composition, the radical reaction between  $n$ -alkenes and H-Si are statistically random.<sup>2,7</sup> This would be expected to produce a mixed monolayer with a similar composition as that in the deposition solution (i.e., without significant domain formation).<sup>13a</sup> In fact, Sieval et al. reported that the Cassie plots of mixed  $n$ -alkyl/amino-terminated alkyl monolayers on silicon are approximately linear, which indicated that the solution and surface compositions are close to each other.<sup>6c</sup>

We also studied mixed monolayers prepared from ethyl undecylenate and  $n$ -alkenes of different chain lengths, keeping the mole fraction of ethyl undecylenate in the solution constant, i.e.,  $\chi_{\text{ester}}(\text{soln}) = 0.5$ . Figure 4 shows the ATR-FTIR spectra of these mixed monolayers, with 1-octyl, 1-decyl, 1-dodecyl, and 1-tetradecyl chains, respectively. The spectral features are similar to those shown in Figure 1, particularly in the two characteristic regions due to the C-H and carbonyl stretching vibrations. The positions of the C-H stretches, i.e.,  $\nu_a(\text{CH}_3)$  at 2958–9  $\text{cm}^{-1}$ ,  $\nu_a(\text{CH}_2)$  at 2920–2  $\text{cm}^{-1}$ , and  $\nu_s(\text{CH}_2)$  at 2850–2  $\text{cm}^{-1}$  are identical within the experimental uncertainty, indicating that these mixed monolayers are also closely packed, and there are no significant differences in terms of chain conformation and orientation.<sup>6,7</sup> This is in contrast to the well-documented chain length dependence of the structure of mixed alkanethiolate monolayers on gold,<sup>41</sup> of which the formation is substantially influenced by the interchain interactions beyond the chemisorption of thiols on gold substrates.<sup>3b</sup>

For comparison, we plotted in Figure 5A the absorbances of  $\nu_a(\text{CH}_2)$  at 2920–2  $\text{cm}^{-1}$  and of  $\nu(\text{C}=\text{O})$  at 1740–3  $\text{cm}^{-1}$

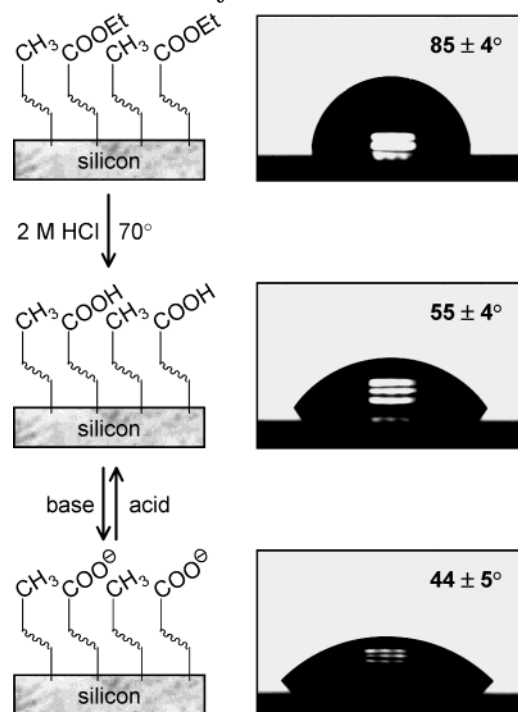


**Figure 5.** (A) Plot of absorbance of  $\nu(\text{C}=\text{O})$  at 1740–3  $\text{cm}^{-1}$  (closed circles) and of  $\nu_a(\text{CH}_2)$  at 2922  $\text{cm}^{-1}$  (open circles) in the ATR-FTIR spectra shown in Figure 4; (B) water contact angles of mixed monolayers before (closed circles) and after hydrolysis in 2.0 M HCl at 70° for 2 h (open circles) vs length of unsubstituted alkyl chains. The dotted lines are included simply to guide the eye.

as a function of the length of the unsubstituted alkyl chains. It is not surprising that the  $\nu_a(\text{CH}_2)$  intensity increases with the number of methylene groups since the surface density of the four mixed monolayers remains almost the same, as mentioned above. However, there are no clear correlations between the absorbance of  $\nu(\text{C}=\text{O})$  and the alkyl chain length, indicating that the number of ester groups introduced to the surface does not depend on the type of  $n$ -alkenes used for dilution.

The wetting measurements (Figure 5B) reveal different trends from the spectroscopic data (Figure 5A). The water contact angles clearly increase with increased alkyl chain length; i.e., the longer the alkyl chains, the more hydrophobic the mixed monolayer becomes. Because the surface density of ester groups remains constant (as indicated by the ATR-FTIR data), this variation of hydrophobicity can only be understood in terms of the microenvironment of the monolayers, particularly the positions of the esters groups with respect to the terminal methyl groups of unsubstituted alkyl chains. When short  $n$ -alkenes (e.g., 1-octene) are used to prepare the mixed monolayers, the undecylenate ester groups protrude above the plane of the methyl groups, while with longer  $n$ -alkenes (e.g., 1-tetradecene) they are buried in the hydrophobic “pockets” created by the long alkyl chains. It has been demonstrated by Bain et al.<sup>42</sup> that in  $\omega$ -alkoxy- $n$ -alkanethiolate mono-

(41) (a) Folkers, J. P.; Laibinis, P. E.; Whitesides, G. M. *Langmuir* **1992**, *8*, 1330–1341. (b) Atré, S. V.; Liedberg, B.; Allara, D. L. *Langmuir* **1995**, *11*, 3882–3893.

**Scheme 2. Schematic Representation of the Formation and Acid–Base Reaction of Mixed Acidic Monolayers on Silicon<sup>a</sup>**

<sup>a</sup> The photographs show a water drop in contact with the silicon surface (a mixed monolayer prepared from equimolar amounts of 1-dodecene and ethyl undecylenate) and the contact angles measured after each step of reaction.

layers on gold wetting measurements are only sensitive to the first few sequential atoms at the air/film interface.

As discussed below, both the mole fraction and alkyl chain length in the mixed monolayers influence the reactivity of the ester groups and the acid–base properties of the COOH groups after hydrolysis. The experimental results described above serve as guidelines for the optimal choice of conditions to minimize the disruption of the alkyl chain packing in the monolayers when reagents are added to modify the ester groups.

**Hydrolysis of  $\omega$ -Ethoxycarbonyl/Alkyl Monolayers on Silicon.** High-quality alkyl monolayers terminated with carboxylic acid (COOH) groups on crystalline silicon cannot be prepared directly since carboxylic acids react with hydrogen-terminated silicon to yield disordered films.<sup>6a,13b,43</sup> Therefore, structurally well-defined COOH-terminated monolayers are commonly prepared by hydrolysis of ester-terminated monolayers on silicon (Scheme 2).<sup>6a,7b,13a,17a</sup>

Under basic conditions (e.g., dipping in 2.0 M KOH for 1 h),  $\omega$ -ethoxycarbonyl-terminated (“ester-terminated”) monolayers on silicon are unfortunately damaged or even destroyed.<sup>2b,7a</sup> Consequently, we made our first attempt with aqueous HCl solution. A similar procedure was initially used to hydrolyze alkanesiloxane monolayers prepared from  $\text{Cl}_3\text{Si}(\text{CH}_2)_{10}\text{COOCH}_3$  on hydroxylated silicon,<sup>23c</sup> and recently adopted to ester-terminated monolayers on silicon.<sup>6a,7b</sup> The ATR-FTIR spectra of the products present upon hydrolysis and subsequent treatment with dilute acid and base are shown in Figure 6.

The spectrum of ethyl undecylenate monolayers on silicon (Figure 6A) features the carbonyl stretch,  $\nu(\text{C}=\text{O})$ ,

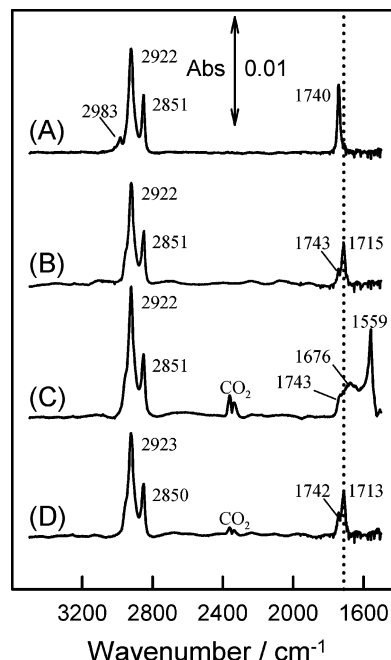


**Figure 6.** ATR-FTIR spectroscopic monitoring of the acid-catalyzed hydrolysis of ethyl undecylenate monolayers on silicon: (A) before hydrolysis; (B) after hydrolysis in 2.0 M HCl at 70 °C for 2 h; (C) after treatment of the hydrolyzed surface with 0.01 M NaOH; (D) sample in panel C after washing with 2 M HCl.

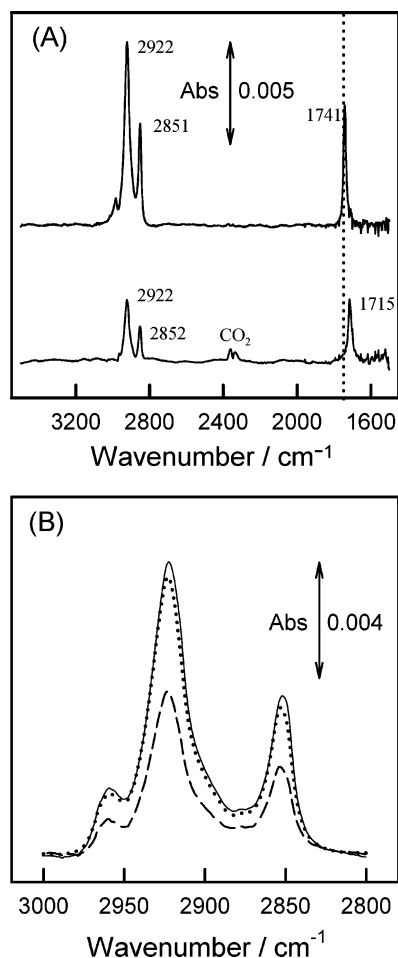
as a sharp and symmetric peak at 1740  $\text{cm}^{-1}$ . After hydrolysis by 2.0 M HCl at 70 °C for 2 h, two overlapping bands at 1743 and 1715  $\text{cm}^{-1}$  are discernible (Figure 6B), and the latter has a much higher intensity. The assignment of the 1715  $\text{cm}^{-1}$  peak to the C=O stretch of the carboxylic acid is straightforward, while the shoulder-band at 1743  $\text{cm}^{-1}$  is difficult to interpret. These results and our experiments with mixed monolayers (see below) indicate that the hydrolysis of the ester groups was not complete, as observed before for the hydrolysis of ester-terminated alkylsiloxane monolayers on hydroxylated silicon.<sup>20</sup> For a similar type of ester-terminated monolayers on silicon surfaces, Sieval et al. also observed two peaks in the carbonyl region, although the low signal-to-noise ratio prevented a clear interpretation.<sup>6a</sup>

Figure 6C,D shows the spectra after treatment of the hydrolyzed surface with dilute base and then acid. Dipping the sample into a dilute base (0.01 M NaOH) readily transformed the carboxylic acid to its salt (Scheme 2) as evidenced by the sharp peak at 1559  $\text{cm}^{-1}$  attributable to the carboxylate anion.<sup>35</sup> Remarkably, the COOH groups on the surface can be regenerated by subsequent washing with HCl (2.0 M), as confirmed by the identical features of spectra 6B,D. It should be noted that spectrum 6C exhibits an additional broad band centered at 1676  $\text{cm}^{-1}$  that we cannot assign at this stage. Another significant feature is the shoulder peak at 1742  $\text{cm}^{-1}$ , which can again be attributed to unreacted ester groups. The acid–base properties of thus formed acidic mixed monolayers will be discussed in detail below.

Another protocol for hydrolysis of ester-terminated monolayers on silicon, reported by Hamers et al.<sup>17a</sup> and Zhao et al.,<sup>13a,19</sup> is based on a general procedure used for

(42) (a) Bain, C. D.; Whitesides, G. M. *J. Am. Chem. Soc.* **1988**, *110*, 5897–5898. (b) Laibinis, P. E.; Bain, C. D.; Nuzzo, R. G.; Whitesides, G. M. *J. Am. Chem. Soc.* **1995**, *99*, 7663–7676.

(43) During the review process of this paper, Boukherroub et al. reported their studies of the direct attachment of  $\omega$ -carboxy-1-alkenes to porous silicon under microwave irradiation (Boukherroub, R.; Petit, A.; Loupy, A.; Chazalviel, J.-N.; Ozanam, F. *J. Phys. Chem. B* **2003**, *107*, 13459–13462, accepted for publication on October 9, 2003) We thank the reviewer for drawing it to our attention.



**Figure 7.** ATR-FTIR spectroscopic monitoring of the stability of 1-dodecyl monolayers on silicon: Solid line = freshly prepared; dotted line = after treatment with 2.0 M HCl at 70 °C for 2 h; dashed line = after dipping into 0.25 M potassium *tert*-butoxide/DMSO solution for 3 min.

hydrolysis of hindered carboxylic esters.<sup>44</sup> The ester groups are first activated by dipping the modified silicon samples into potassium *tert*-butoxide solution in DMSO for 3 min, and then washed with 2.0 M HCl solution. In Figure 7, the top spectrum shows the features of the original, the bottom spectrum those of the hydrolyzed monolayers. The disappearance of the ester carbonyl stretch at 1741  $\text{cm}^{-1}$  and the ethoxy  $\text{CH}_3$  stretch at 2983  $\text{cm}^{-1}$  and, more importantly, the appearance of a sharp band at 1715  $\text{cm}^{-1}$  demonstrate unambiguously the complete hydrolysis. Although this approach is very favorable in terms of the hydrolysis efficiency, it should be noted that the intensities of the  $\text{CH}_2$  stretching bands decreased considerably. As a control experiment, we compared these two hydrolysis protocols by using inert 1-dodecyl monolayers on silicon. As shown in Figure 7B, treatment with 2 M HCl at 70 °C for 2 h led to a drop of the  $\nu_{\text{a}}(\text{CH}_2)$  intensity by less than 5%, while immersion in 0.25 M potassium *tert*-butoxide solution in DMSO for only 3 min accounted for more than 50% loss of hydrocarbon chains from the silicon surface; i.e., the monolayer structure is severely damaged by the strong base. The instability of alkyl monolayers on silicon under basic conditions has been observed previously;<sup>2b,7a</sup> we believe it is due to the reactivity of the substrate toward base.

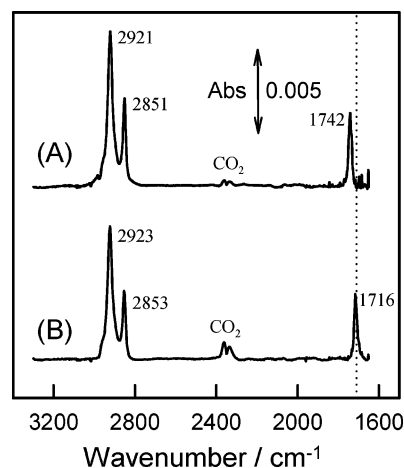


**Figure 8.** ATR-FTIR spectroscopic monitoring of the hydrolysis of mixed monolayers prepared from 1-dodecene and ethyl undecylenate in solution. (A) Before hydrolysis ( $\chi_{\text{ester}}(\text{soln}) = 0.75$ ); (B) after treatment with 2.0 M HCl at 70 °C for 2 h ( $\chi_{\text{ester}}(\text{soln}) = 0.75$ ).

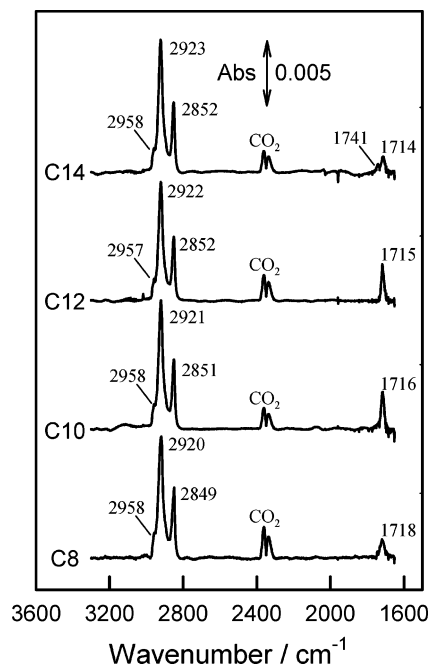


**Figure 9.** ATR-FTIR spectra of mixed monolayers on silicon prepared from ethyl undecylenate and *n*-alkenes with different chain lengths, after hydrolysis with 2.0 M HCl at 70 °C for 2 h ( $\chi_{\text{ester}}(\text{soln}) = 0.50$  for all cases). C8, C10, C12, and C14 are used as abbreviations for 1-octyl, 1-decyl, 1-dodecyl, and 1-tetradecyl chains, respectively.

We also explored the hydrolysis of the mixed monolayers on silicon in order to gain further insights into the correlation between monolayer structure and reactivity of the modified surfaces. Initially, monolayers prepared from a mixture of ethyl undecylenate and 1-dodecene at different molar ratios were examined. Figure 8 shows that on dilution of ethyl undecylenate with 1-dodecene (e.g.,  $\chi_{\text{ester}}(\text{soln}) = 0.75$ ), the hydrolysis with 2.0 M HCl at 70 °C for 2 h is complete. The ester carbonyl band at 1743  $\text{cm}^{-1}$  vanishes and a distinct  $\text{COOH}$  peak appears at 1716  $\text{cm}^{-1}$ .

We then studied the hydrolysis of mixed monolayers prepared from equimolar mixtures of ethyl undecylenate and *n*-alkenes with different chain lengths. Figure 9 shows the ATR-FTIR spectra after hydrolysis in 2.0 M HCl at 70 °C for 2 h. The spectra of C8, C10, and C12 monolayers

(44) (a) Chang, F. C.; Wood, N. F. *Tetrahedron Lett.* **1964**, 2969–2973. (b) Gassman, P. G.; Schenk, W. N. *J. Org. Chem.* **1977**, 42, 918–920.



are not different from that of 1-dodecene/ ethyl undecylenate with  $\chi_{\text{ester}} = 0.75$  (Figure 8), showing a single band at 1715–1718 but no significant absorbance at the carbonyl stretching frequency of ester groups. Interestingly, the carbonyl regions in the spectra of the hydrolyzed products of mixed monolayers formed from 1-tetradecene (C14 in Figure 9) and from pure ethyl undecylenate (Figure 6B) look very similar: both feature two overlapped bands at 1741 and 1714  $\text{cm}^{-1}$ . This can be understood in terms of the varied microenvironment of ester groups within the monolayers as mentioned above. The undecylenate ester groups protrude above the plane of shorter alkyl chains (C8, C10, C12), making them accessible for hydrolysis, but they are buried underneath the ends of hydrophobic long chains (C14), which make them less accessible.

The hydrolysis of ester-terminated monolayers on silicon was also monitored by wetting measurements (Scheme 2). A significant decrease of water contact angles was observed as shown in Figures 3A and 5B, indicating the formation of hydrophilic acid groups on the surfaces upon hydrolysis. For the monolayers prepared from pure ethyl undecylenate, the water contact angles also decreased upon hydrolysis, but different from the behavior of structurally well-defined  $\omega$ -carboxylic acid terminated monolayers on gold prepared by direct adsorption of  $\text{HS}-(\text{CH}_2)_n\text{COOH}$  from solution.<sup>24c,29a</sup> In the latter case, the advancing contact angles of water are essentially zero ( $<20^\circ$ ),<sup>29a</sup> significantly lower than those obtained on acidic monolayers on silicon ( $44 \pm 5^\circ$ ) prepared via hydrolysis. The difference suggests that the exposed interface consists not only of hydrophilic COOH groups but also of some more hydrophobic species, e.g., unreacted ester groups.

The hypothesis of incomplete hydrolysis of monolayers on silicon prepared from pure ethyl undecylenate is supported by the results of our studies of mixed monolayers at different molar ratios and with different alkyl chain lengths, and by wetting measurements. However, further confirmation is desirable, e.g., by replacing the ethyl ester of undecylenic acid by the trifluoroethyl ester to achieve a better separation of the two carbonyl bands.<sup>35</sup> In addition, the deviation of the surface composition determined by ATR-FTIR from that determined by wetting measurements (Cassie's Law) requires reexamination with other experimental techniques.

**Contact Angle Titrations of the Hydrolyzed Monolayers on Silicon.** To measure the acid–base properties of the mixed monolayers on silicon upon hydrolysis quantitatively, we decided to do contact angle titrations (i.e., determination of contact angles as a function of pH), as motivated by previous examples on other surfaces.<sup>22,23c,27–28</sup> However, two essential issues must be addressed prior to the acquisition and analysis of the contact angle data for mixed monolayers on silicon, namely the sample pretreatment and the determination of acid dissociation constants on surfaces (surface  $\text{p}K_a$ ) from the experimentally obtained titration curves. It has been demonstrated that contact angle titration curves on acidic alkanethiolate monolayers on gold are sensitive to the sample pretreatment.<sup>27a,28</sup> We find that prior to the measurement of contact angles, the silicon sample must be immersed in a pH-matched solution (the nonreactive spreading protocol<sup>28</sup>) and then dried with  $\text{N}_2$ , to produce a titration curve with clearly defined plateau regions at high and low pH and a smooth transitional region at intermediate pH. It has been postulated that this pretreatment leaves the surface in a partially deprotonated state even though it is not macroscopically wet. This has been confirmed for the mixed *n*-alkanoic acid/alkyl mono-

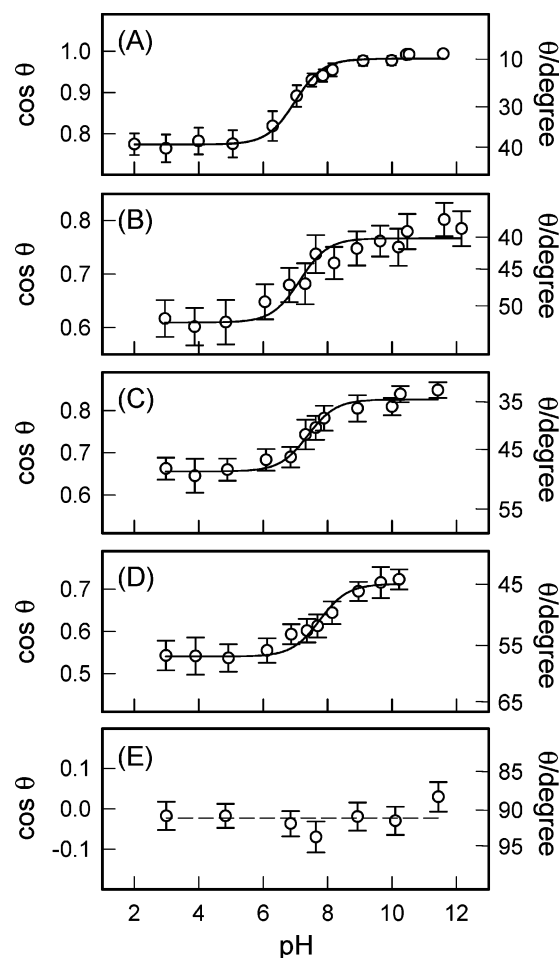


**Figure 10.** Contact angle titration curves measured using the nonreactive spreading protocol for mixed acidic monolayers on silicon prepared from mixtures of 1-dodecene and ethyl undecylenate of varied composition upon hydrolysis (2.0 M HCl at 70 °C for 2 h). The mole fractions of ethyl undecylenate in the deposition solutions ( $\chi_{\text{ester}}(\text{soln})$ ) are (A) 1.0, (B) 0.75, (C) 0.50, (D) 0.25, and (E) 0, respectively.

layers on silicon by our ATR-FTIR studies (appearance of a carbonate peak, Figure 6C). The cosine of the contact angle at a given pH can be expressed as<sup>28</sup>

$$\cos \theta = \cos \theta_{\text{lowpH}} + \alpha(\chi_{\text{acid}})(\cos \theta_{\text{deprotacid}} - \cos \theta_{\text{protacid}}) \quad (3)$$

where  $\chi_{\text{acid}}$  is the mole fraction of carboxylic acid groups on the surface (obtained from FTIR data, see above) and  $\theta_{\text{lowpH}}$  is the contact angle at a pH at which all the acidic sites are protonated. The term  $\alpha$  is the fraction of dissociation of the surface carboxylic acid moieties at a given pH, which can be derived from the rearranged formula for a monoprotic acid dissociation equilibrium:<sup>27a</sup>

$$\alpha = \frac{10^{\text{pH}-\text{p}K_a}}{1 + 10^{\text{pH}-\text{p}K_a}} \quad (4)$$

The contact angle titration curves shown in Figure 10 correspond to the mixed monolayers on silicon formed by the reactions of H–Si with solutions containing ethyl undecylenate and 1-dodecene at different molar ratios after hydrolysis in 2.0 M HCl. The uncertainties shown for each data point are the standard deviations of multiple measurements: each of the titration curves was reproduced at least three times using three independently

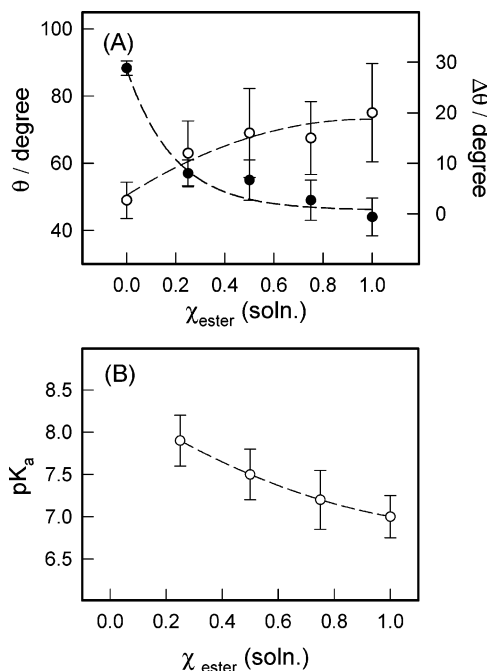


**Figure 11.** (A) Contact angles at low pH (closed circles) and contact angle differences between plateau regions at low and high pH (open circles); (B) surface acid dissociation constant,  $pK_a$ , as a function of the mole fraction of ethyl undecylenate in solution,  $\chi_{\text{ester}}$  (soln.). The dashed lines are included simply to guide the eye.

prepared samples. To confirm that the titration curves are not artificial due to the instability of alkyl monolayers on silicon in basic solution, pure 1-dodecyl monolayers were examined in control experiments (Figure 10E). Despite the different surface compositions, all the surfaces bearing carboxylic acid groups exhibited typical titration curves. As shown in Figures 10A–D, the titration curves are sigmoidal with two well-defined plateau regions at low and high pH and a smooth transition in between. In particular, the titration curve of hydrolyzed monolayers prepared from pure ethyl undecylenate (Figure 10A) did not show a “hump”, i.e., lower wettability at intermediate pH values, a phenomenon observed for 11-mercaptopundecanoic acid monolayers on gold.<sup>27b</sup> This is probably due to the incomplete ester hydrolysis yielding mixed carboxylic acid/ester terminated monolayers, in which the formation of hydrogen bonds between carboxylic acid groups and neighboring carboxylate anions is not feasible.<sup>27b</sup>

Figure 11 shows that the contact angle at low pH decreases upon increasing the mole fraction of ethyl undecylenate in the deposition solution. This indicates that as the concentration of COOH groups increases, the monolayers become more hydrophilic as expected. Meanwhile, the difference between the plateau regions increases monotonically, although the experimental uncertainties were rather large. The determination of the plateau value at high pH is somewhat problematic, which may be due to the instability of the monolayers under basic conditions. To minimize any systematic error, we measured the contact angles for pH = 1–11 in random order, those for pH 12 and higher last.

To quantitatively understand the acid–base properties of the mixed monolayers, we fit the experimental data with the help of equations (3) and (4). The  $\cos \theta_{\text{lowpH}}$  was determined from the average of the experimental data, typically the first four points at low pH.  $\chi_{\text{acid}}$  on surface was obtained from the FTIR data shown in Figure 2.  $\cos$

$\theta_{\text{protacid}}$  was calculated from the  $\cos \theta_{\text{lowpH}}$  using Cassie's approximation.<sup>40,45</sup> However, the determination of  $\cos \theta_{\text{deprotacid}}$  is somewhat arbitrary, partially because of the large uncertainty associated with the contact angles at high pH as mentioned above. Nevertheless, we could fit this value and  $pK_a$  simultaneously, thereby obtaining more accurate  $pK_a$  values than by simple estimation of the inflection points in the titration curves.<sup>23c,27–28</sup> Figure 11B illustrates that the surface  $pK_a$  increases with decreasing surface concentration of carboxylic acid groups, i.e., from  $pK_a = 7.0 \pm 0.3$  for  $\chi_{\text{ester}}(\text{soln}) = 1.0$  to  $pK_a = 7.9 \pm 0.3$  for  $\chi_{\text{ester}}(\text{soln}) = 0.25$ . It should be noted that all these values are significantly higher than the  $pK_a$  of *n*-nonanoic acid (pelargonic acid, the closest representative *n*-alkanoic acid found in the literature) of 4.94 in aqueous solution at 25 °C.<sup>46</sup>

Wasserman et al. have reported similar surface concentration effects for contact angle titrations of alkylsiloxane monolayers (on hydroxylated silicon) containing both methyl and carboxylic acid groups.<sup>23c</sup> Similar to the present work, a substantial  $pK_a$  increase (from 7.0 to 11) was observed when the surface coverage of COOH groups decreased from 100% to 20%. For mixed  $\omega$ -mercaptopundecanoic acid/undecanethiol monolayers on gold, Lee et al. reported similar features of the contact titration curves (i.e., dependence on the surface concentration of COOH, but no quantitative assessment of the  $pK_a$  variations).<sup>27b</sup> Creager and Clarke varied the molar ratio of 11-mercaptopundecanoic acid and undecanethiol from 1:2 to 5:1. Of the two monolayers that exhibited well-defined titration curves (1:2 and 1:1), the former had a slightly lower  $pK_a$ .<sup>28</sup> It should be noted that the mole fraction of carboxylic acid groups in those mixed alkanethiolate monolayers does not mirror the solution composition, as a result of the preferred adsorption of *n*-alkanethiols over  $\omega$ -substituted alkanethiols to gold.<sup>42</sup>

We also studied the acid–base properties of mixed monolayers prepared from ethyl undecylenate and *n*-alkenes of different chain lengths upon hydrolysis. Figure 12 presents the contact angle titration curves for hydrolyzed monolayers on silicon that were prepared from equimolar mixtures of ethyl undecylenate and 1-octene (C8), 1-decene (C10), 1-dodecene (C12) and 1-tetradecene (C14), respectively. Our FTIR spectra have shown that the surface density of ester groups does not change appreciably, but their accessibility to hydrolysis is different, particularly for the longer chains. The contact angle titration curves of the hydrolyzed monolayers (Figure 12) are in fact very similar to those shown in Figure 10A–D; they all exhibit typical plateau regions at low and high pH, and clear transitions at intermediate pH values. As shown in Figure 13A, the initial contact angle becomes larger when the length of the unsubstituted alkyl chain increases, as expected for increased hydrophobicity. However, the contact angle differences between the two plateau regions did not change significantly, supporting the hypothesis that the surface concentration of acid groups remains nearly constant.

The surface  $pK_a$  values for these monolayers were determined as described above and are plotted in Figure 13B. They clearly increase with increasing length of the

(45) Although the surface composition obtained from the contact angle data according to Cassie's equation is not consistent with that determined from spectroscopic measurements, the calculations of  $\cos \theta_{\text{protacid}}$  and  $\cos \theta_{\text{lowpH}}$  should be reasonably accurate for the purpose of fitting experimental data to obtain  $pK_a$  values, particularly since the surface composition is known from the spectroscopic studies.

(46) Rappoport, Z. *Handbook of Tables for Organic Compound Identification*, 3rd ed.; The Chemical Rubber Co.: Cleveland, OH, 1967; p 432.

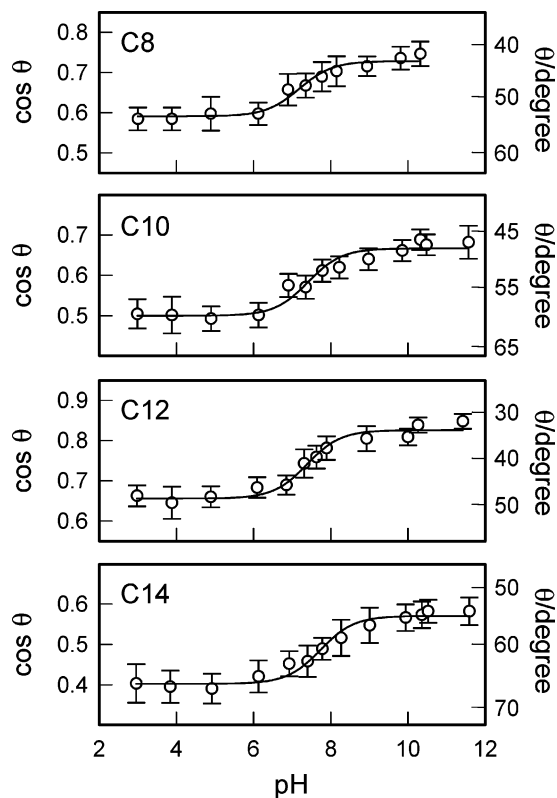


**Figure 12.** Representative contact-angle titration curves measured for mixed monolayers on silicon prepared from equimolar mixtures of ethyl undecylenate with 1-octene (C8), 1-decene (C10), 1-dodecene (C12), and 1-tetradecene (C14) after hydrolysis in 2.0 M HCl at 70 °C for 2 h.

unsubstituted alkyl chain. The shift from 1-octyl ( $pK_a = 7.2 \pm 0.3$ ) to 1-tetradecyl ( $7.8 \pm 0.3$ ) monolayers is only 0.6 pK units, considerably smaller than that shown in Figure 11B. Nevertheless, the trend is consistent with the much larger  $pK_a$  shift (up to 5.2 pK units) observed for a series of mixed monolayers on gold formed by coadsorption of 11-mercaptoundecanoic acid and 1-nonanethiol, 1-decanethiol, 1-undecanethiol, and 1-dodecanethiol, respectively.<sup>28</sup>

From the contact angle titration results described above and their comparison with literature data, it is clear that the surface  $pK_a$  depends on the structure and composition of the mixed monolayers on silicon. However, the  $pK_a$  shifts on silicon are not as significant as those observed for alkylsiloxane monolayers on hydroxylated silicon and alkanethiolate monolayers on gold.<sup>23c,28</sup> Our results are in consistent with the fact that surface  $pK_a$  values of short-chain  $\omega$ -mercaptoalkanoic acid/alkanethiol monolayers on gold (which are believed to have relatively low packing density and disordered structures) are almost independent of the alkanethiol chain lengths.<sup>28</sup>

In the past, the decrease in the acidity of the carboxyl groups upon increasing the mole fraction of unsubstituted alkyl groups<sup>23c</sup> and the chain length of  $n$ -alkanethiols<sup>28</sup> within the mixed monolayers has been attributed to the placement of the acid moiety in an increasingly nonpolar and hydrophobic microenvironment. We believe this also holds true for the mixed monolayers on silicon. At least two different effects may be responsible for the observed  $pK_a$  shifts: ion solvation energetics in the interfacial microenvironment and the interfacial potential at the monolayer surface.<sup>28</sup> In particular, a positive  $pK_a$  shift with increasing either the mole fraction of 1-dodecyl chains or the length of  $n$ -alkyl chains is expected if the  $n$ -alkyl

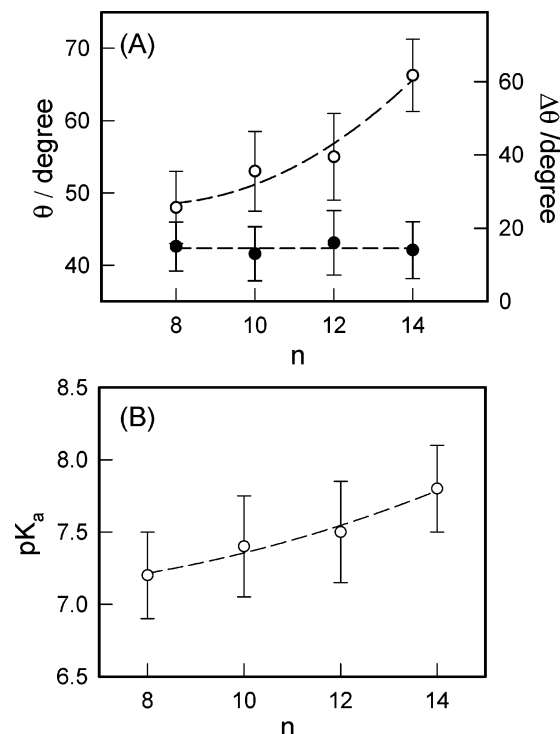


**Figure 13.** (A) Contact angles at low pH (open circles) and contact angle differences between plateau regions at low and high pH (closed circles); (B) surface acid dissociation constant,  $pK_a$ , as a function of the length of unsubstituted alkyl chains within the mixed monolayers. The dashed lines are included simply to guide the eye.

chains create “hydrophobic pockets” around the carboxylic acid groups in which the solvation of carboxylate anions is disfavored. The situation is similar to the observed  $pK_a$  shifts for  $n$ -alkanoic acids in organic media<sup>47</sup> and for steric congestion around carboxylate groups.<sup>48</sup> Such an effect can be theoretically understood on the basis of the Born model by considering the differences of the dielectric constants at the surface and in the bulk solution,<sup>49</sup> providing that the ideal dielectric properties of alkyl monolayers on silicon have been previously confirmed.<sup>11a,13a</sup> An interfacial potential effect also may be present, although we would expect a lower  $pK_a$  value (i.e., closer to that in aqueous solutions) as a result of the decreased surface charge density when the mole fraction of acid groups decreases.<sup>28</sup> The weak  $pK_a$  dependence probably results in a fortuitous balancing of the effects of local dielectric constant (tending to increase the  $pK_a$  with decreasing mole fraction of the acid groups) and surface charging. Due to the lower packing density of the mixed monolayers on silicon, the surface charge density for the system under study should be substantially lower than that of alkanethiolate monolayers on gold.

Further discussion and investigations are desirable to determine the origin of the observed  $pK_a$  shifts but are beyond the scope of this report. We wish to emphasize that the knowledge of accurate surface  $pK_a$  values and their shifts from aqueous solutions is essential for the evaluation of ionization states of the carboxyl groups on silicon surfaces. As shown in eq 4, the fraction of dissociation of COOH groups on the surface depends on

(47) Izutsh, K. *Acid–Base Dissociation Constants in Dipolar Aprotic Solvents*; Blackwell: London, 1990.

(48) Hammond, G. S.; Hogle, D. H. *J. Am. Chem. Soc.* **1955**, *77*, 338–340.

(49) Conway, B. E. *J. Solution Chem.* **1978**, *7*, 721–770.



the surface  $pK_a$  and the pH of the solution. According to the desired derivatization strategy, optimal pH values should be maintained. For example, if the attachment of functional groups is based on electrostatic interactions,<sup>17a,19</sup> a significantly higher pH than the  $pK_a$  value should be chosen in order to achieve complete deprotonation of the carboxylic acid groups. If, on the other hand, amide bonds are to be formed by condensation reaction with the amino groups of macromolecules, the pH should be kept much lower than the surface  $pK_a$ .

### Conclusions

ATR-FTIR Spectroscopy studies and wetting measurements reveal that mixed monolayers prepared by photochemical reaction of hydrogen-terminated silicon (111) with mixtures of *n*-alkenes and ethyl undecylenate exhibit oriented and closely packed structures. The surface density of ester groups can be controlled, as it is predictable from the nearly linear correlation between mole fractions in solution and on the surface. The efficiency of ester hydrolysis under acidic conditions is significantly influenced by the monolayer structure, i.e., the surface density of ester groups and the length of the unsubstituted alkyl chains. Potassium *tert*-butoxide in DMSO hydrolyzes all ester groups but also damages the monolayers.

Mixed acidic monolayers on silicon exhibit typical acid–base properties. Their contact angle titration curves are well defined with two distinct plateau regions at low and high pH, respectively, and a smooth transition at intermediate pH. The surface  $pK_a$  values increase with increasing hydrophobicity of the interface, i.e., by increasing either the mole fraction or the length of the unsubstituted alkyl chains. The  $pK_a$  shifts can be explained by changes in the microenvironment around the acidic groups within the monolayers.

These experimental observations provide fundamental knowledge for the preparation of bio-reactive semiconductor surfaces with controlled and predictable functionality toward further immobilization of biological macromolecules. Progress along this direction will have a major impact on future molecular electronics, sensor, and biochip technology.

**Acknowledgment.** The authors are grateful to the Natural Science and Engineering Research Council of Canada (NSERC) and Simon Fraser University for financial support. H.Z.Y. wishes to thank Dr. Eberhard Kiehlmann for his critical reading of the manuscript and many helpful discussions.

LA035813Q